**Substituent Effects on the Photophysics of the Kaede Chromophore**

Anam Fatima, Giovanni Bressan, Eleanor K. Ashworth, Philip C. B. Page, James N. Bull* and Stephen R. Meech*

*School of Chemistry, University of East Anglia, Norwich NR4 7TJ, UK*

*Authors for Correspondence: s.meech@uea.ac.uk; james.bull@uea.ac.uk

Contents

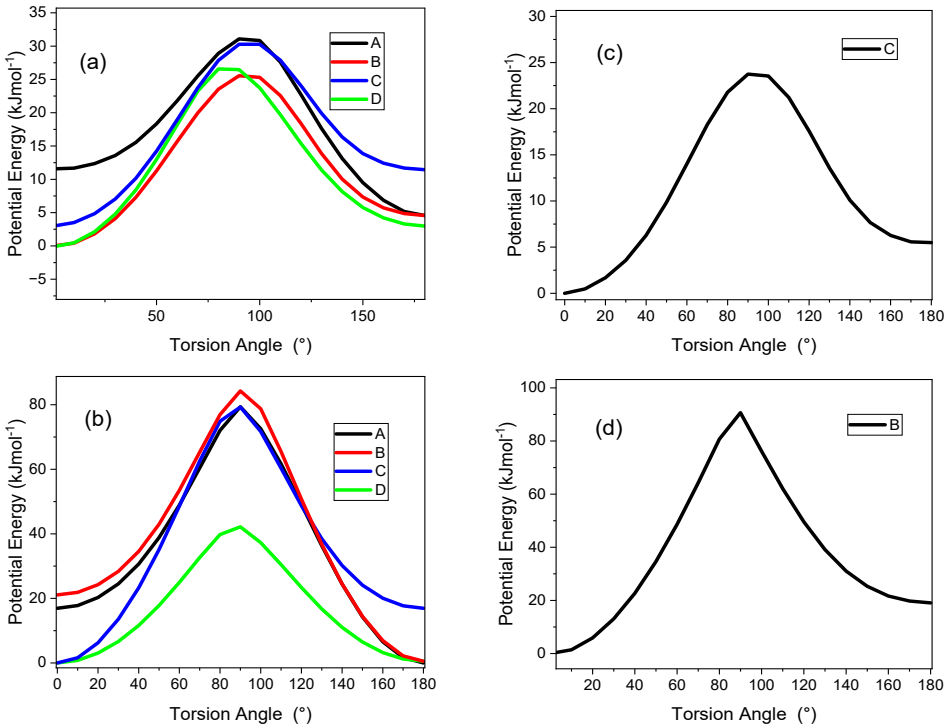


Figure S1. Calculated potential energy surfaces (ωB97X-D/aug-cc-pVDZ level of theory) for torsion about A and B bonds (see Figure 1 in the manuscript). Conformers C and D correspond to torsion about A and B, starting from the alternative conformer of the non-rotating bond. (a) **1** ($S_0$), (b) **1** ($S_1$), (c) **3** ($S_0$), and (d) **4** ($S_1$). Potential energy surfaces for **2** are very similar to 1. In all cases, ground electronic state ($S_0$) barriers are 20—25 kJ $mol^{-1}$ (relative to lowest energy starting isomer). On the other hand, excited state barriers ($S_1$ electronic state) are larger at 40—90 kJ $mol^{-1}$. These are gas phase calculations; relative energies of the conformations and barriers may be influenced by solvation. However, these calculations are consistent with our arguments of multiple conformations in solution exist for **1** and **2**.

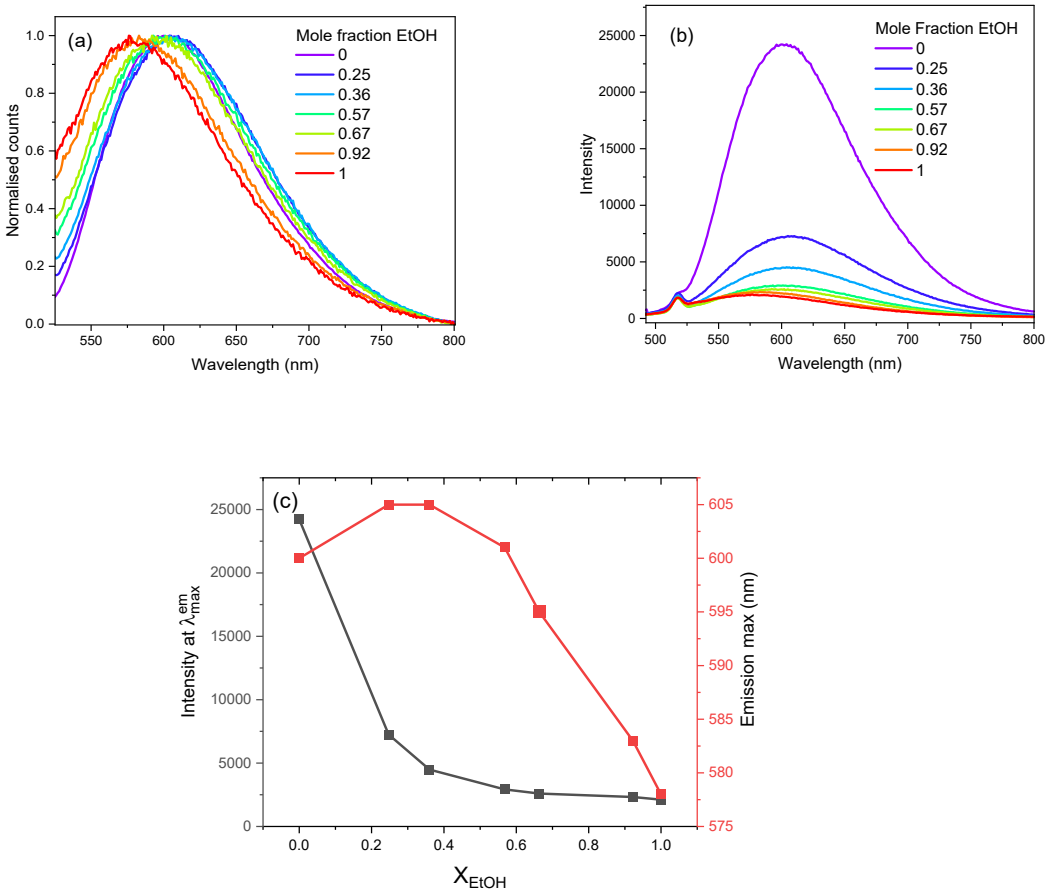


Figure S2. Solvent quenching effect studied for **3** in THF/EtOH mixtures. (a) Normalised emission spectra showing an initial red shift in emission until $x_{EtOH}$= 0.36 followed by an increasing blue shift to $x_{EtOH}$=1. (b) Emission spectra highlighting the decrease in fluorescence quantum yield until $x_{EtOH}$= 0.36 where the quenching is ≈90% complete, and (c) Summary of the solvent quenching and spectral shifts as a function of $x_{EtOH}$.

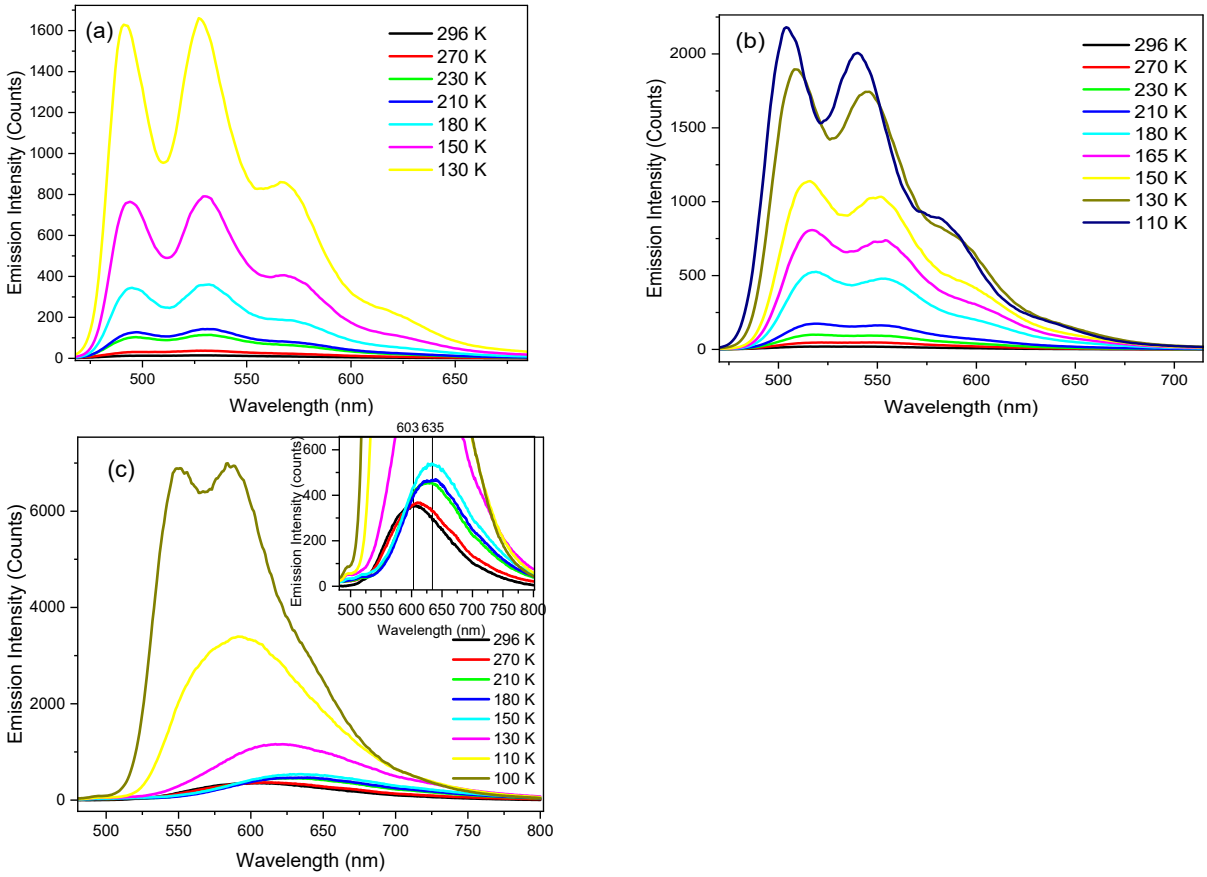


Figure S3. Temperature-dependent emission spectra for: (a) **1** and (b) **2** in ethanol and (c) **3** in 2MTHF as a function of temperature. The inset in (d) highlights the initial red shift in the emission spectra until *T* = 210K.

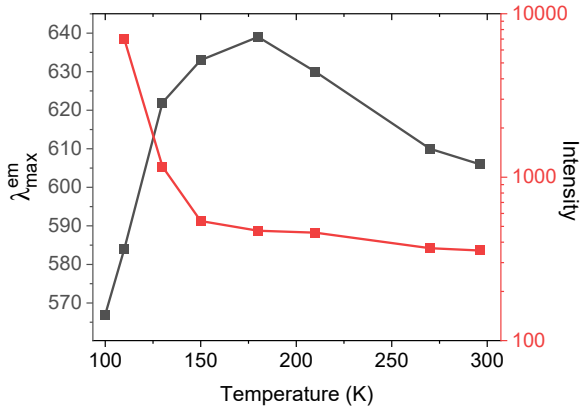


Figure S4. Emission intensity and wavelength as a function of temperature of **3** in 2MTHF. The shape of the curves indicates a biphasic temperature dependence. For intensity, red, an initial slower increase as the temperature is decreased but accelerated for *T*<150 K. Emission spectral shift (black) shows on cooling an initial red shift until *T*=210 K, followed by a blue shift at lower temperatures.

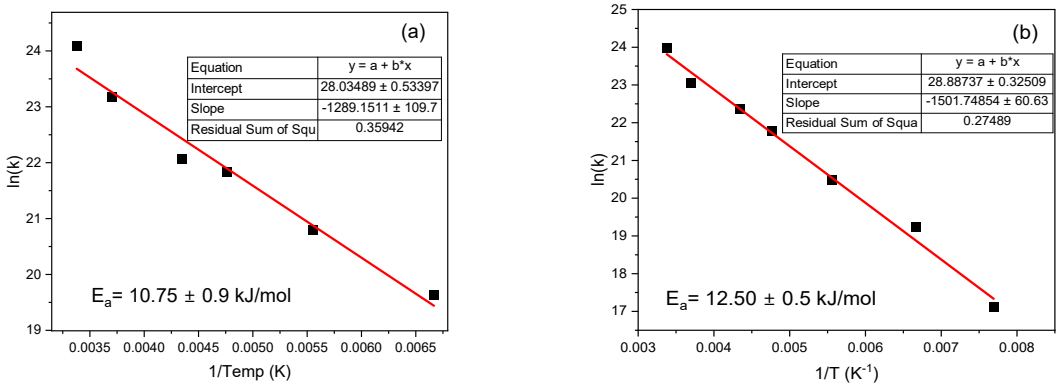


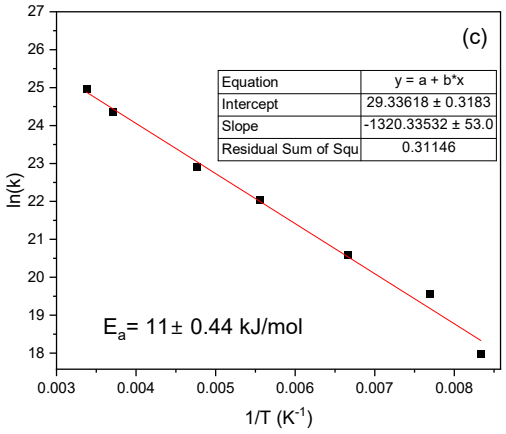

Figure S5. Arrhenius plots (ln ($k_{nr}$) vs. $T^{-1}$) obtained for **1** - **3** in ethanol assuming a single dominant non-radiative decay rate ($k_{nr}$), determined using $k_{nr} = k_r\left(\frac{1}{\varphi_f} - \frac{1}{\varphi_f^0}\right)$, where $k_r$ is the radiative decay rate and $\varphi_f^0$ is the limiting fluorescence quantum yield at low temperature.

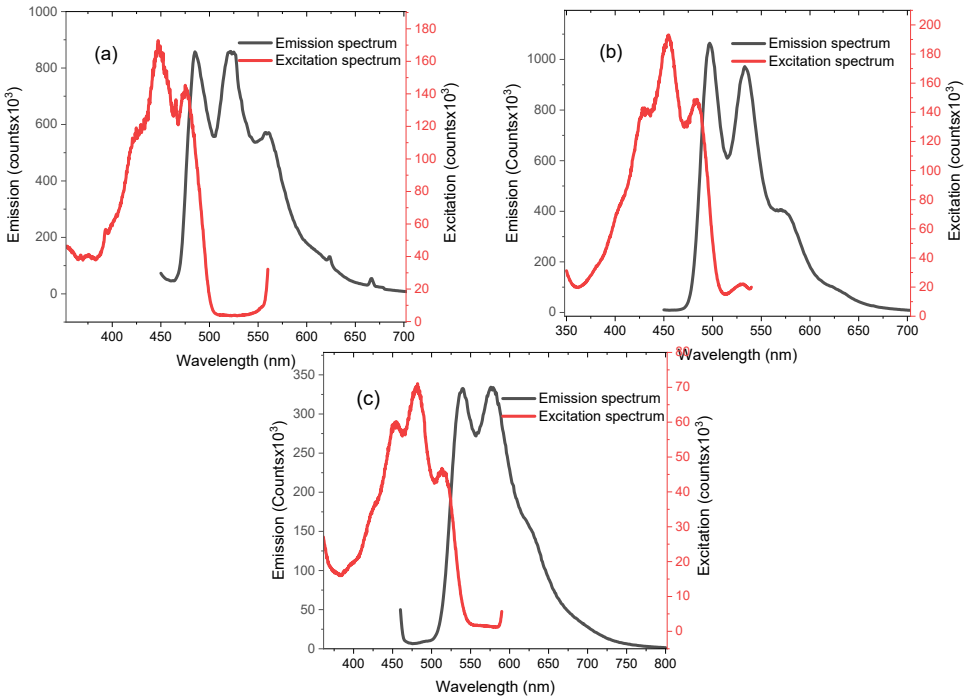


Figure S6. The fluorescence excitation and emission spectra in ethanol at $T$ = 77 K: (a) **1**, (b) **2**, and (c) **3.** The spectra exhibit vibronic structure associated with the $S_0 \leftarrow S_1$ transition, with some degree of a mirror-image relation between fluorescence and absorption.

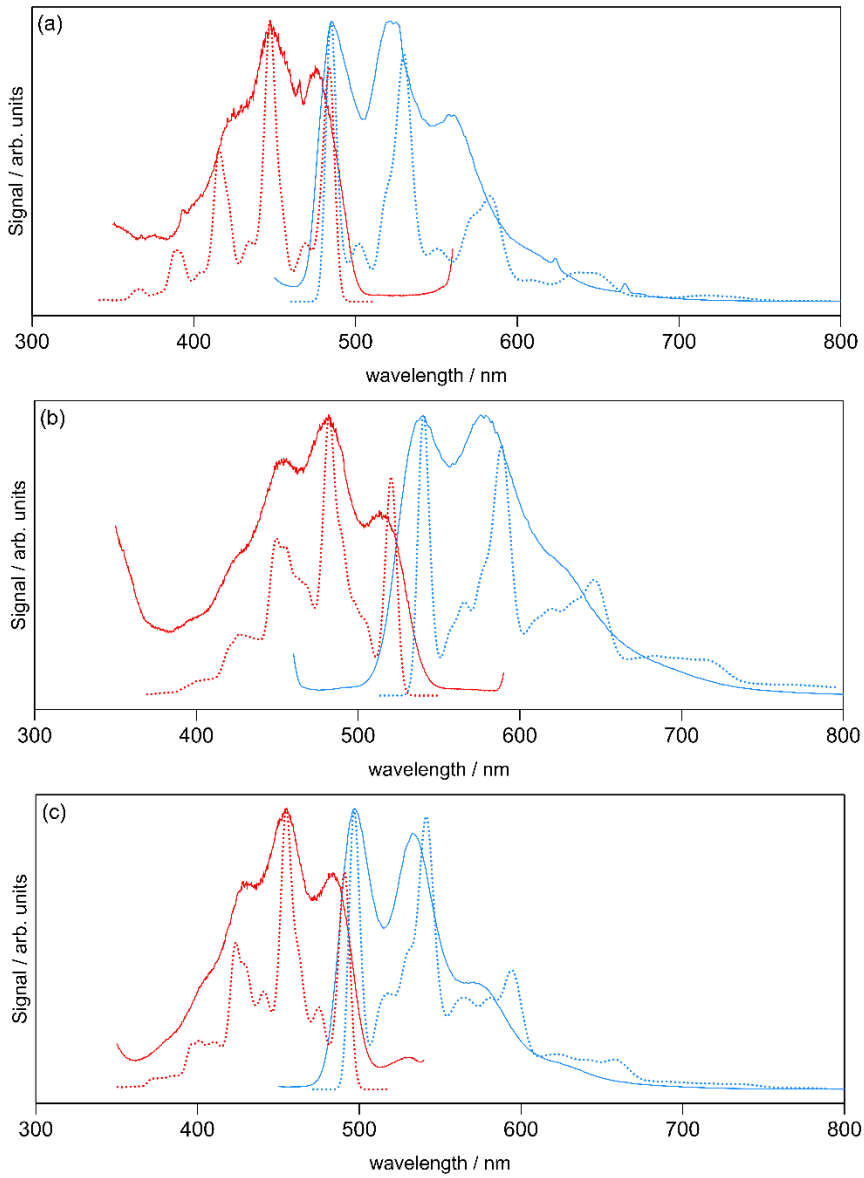


Figure S7. Franck-Condon-Herzberg-Teller (FCHT) simulation of absorption (red) and emission (blue) spectra assuming $T$ = 77 K (dashed lines) compared with experiment (solid lines): (a) **1**, (b) **2**, (c) **3**. Each simulated line was convoluted with a 135 $cm^{-1}$ FHWM Gaussian function, and were all summed to produce the total simulated spectrum. The simulations were translated so that that the maximum had the same wavelength as the experimental spectrum. The translations correspond to (a) 16 nm (abs) and 17 nm (ems) , (b) 3 nm (abs) and 21 nm (ems), and (c) 6 nm (abs) and 3 nm (ems). The FCHT simulation reproduces the non-mirror image symmetry of the absorption-emission profiles.

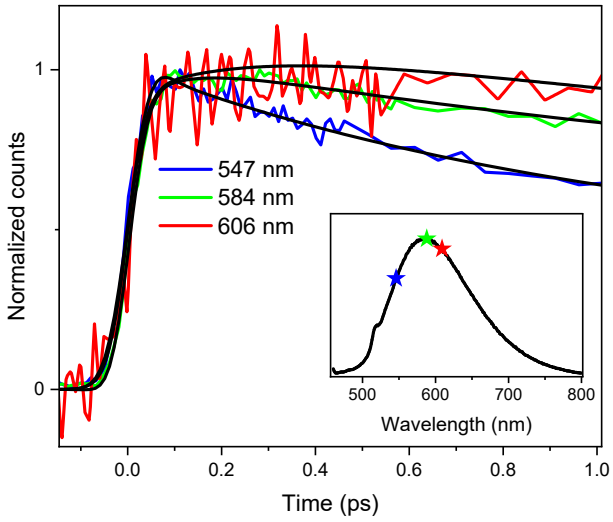


Figure S8. Fluorescence decay of **3** in EtOH recorded using femtosecond fluorescence up-conversion. Fluorescence emission monitored at three wavelengths as indicated in the inset, and the risetime indicated at the red side of the spectrum.

Table S1. Fluorescence up-conversion lifetimes ($\tau$) with the associated pre-exponential factors ($\alpha$) and percentage contributions (wt%) for nitro-Kaede in EtOH at three wavelengths. $\langle\tau_m\rangle$ corresponds to amplitude weighted average lifetime.

| Emission wavelength (nm) | $\alpha_1$ (wt.%) | $\tau_1$/ps | $\alpha_2$ (wt.%) | $\tau_2$/ps | $\alpha_3$ (wt.%) | $\tau_3$ /ps | $\langle\tau_m\rangle$ /ps |
|---|---|---|---|---|---|---|---|
| 547 | 32 (47.0) | 0.9 | 26 (38.2) | 5 | 10 (14.7) | 22 | 6 |
| 584 | -0.2 (0.10)[a] | 0.08 | 118 (57.0) | 4.6 | 89 (42.9) | 19.0 | 10 |
| 606 | -0.32 (2.8)[a] | 0.05 | 11 (97) | 8 | -- | -- | 8 |

[a]negative pre-exponential factors indicate a rising component required to satisfactorily fit the decays at 584 and 606 nm.

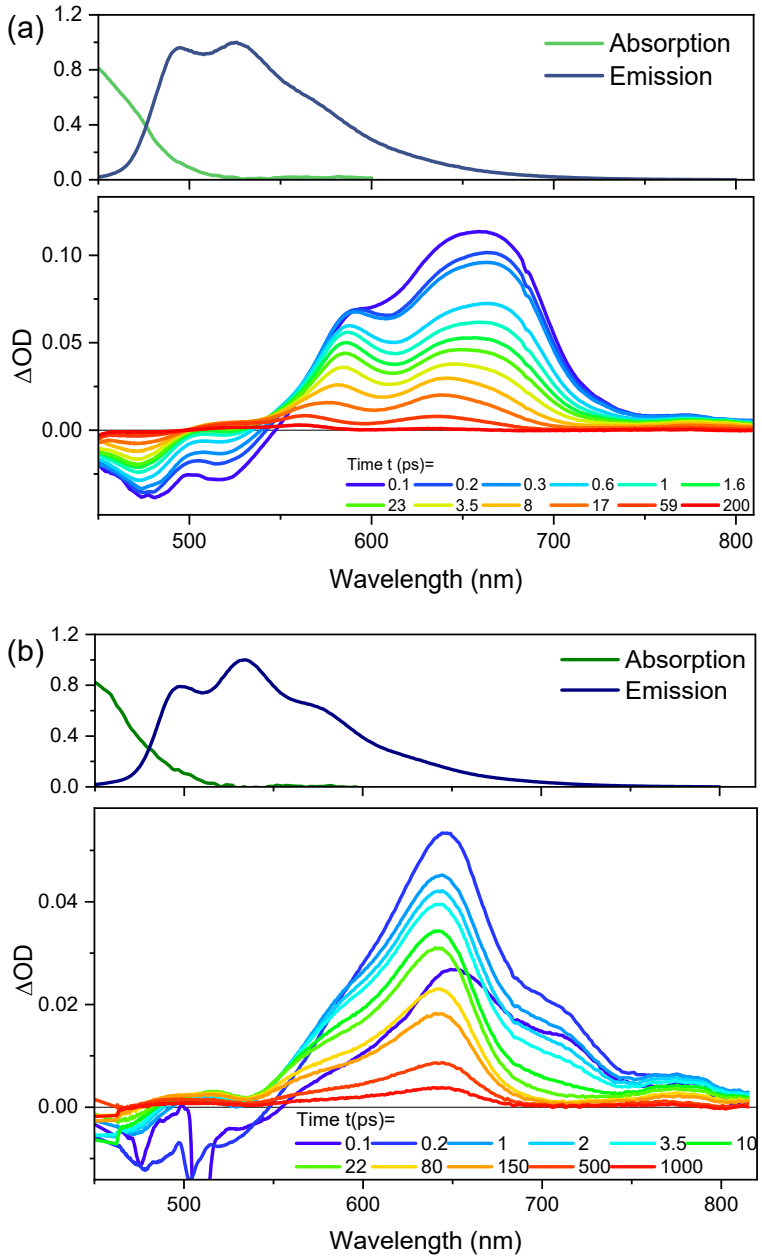


Figure S9. Transient absorption spectra recorded at a series of pump-probe delay times for (a) **1** in EtOH, and (b) **1** in THF. Steady-state absorption and emission spectra are shown for comparison of GSB and SE.

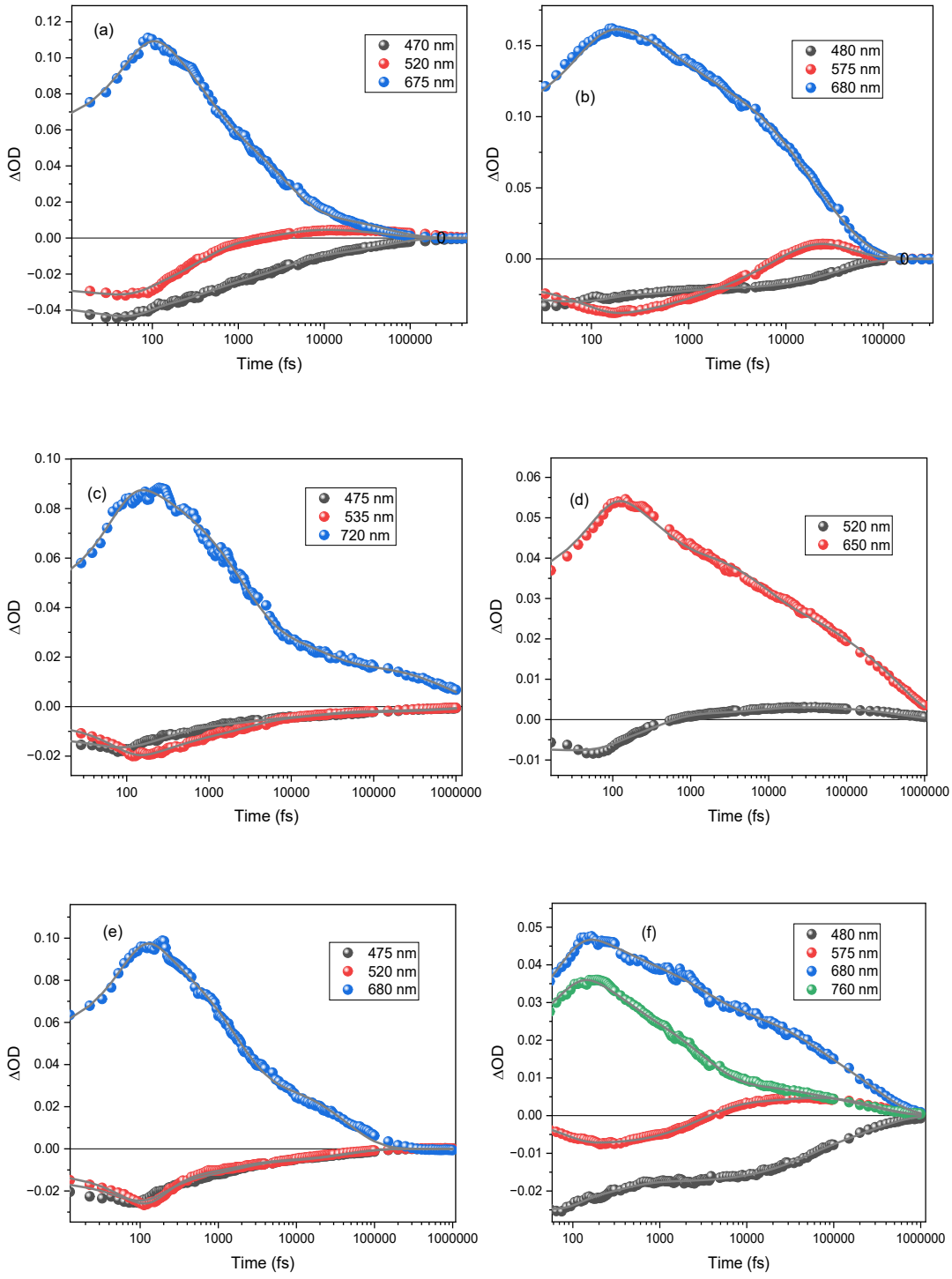


Figure S10. Global biexponential fit of kinetic traces of (a) **1** (b) **2** and (c) **3** in ethanol and (d) **1**, (e) **2** and (f) **3** in THF at selected wavelengths.

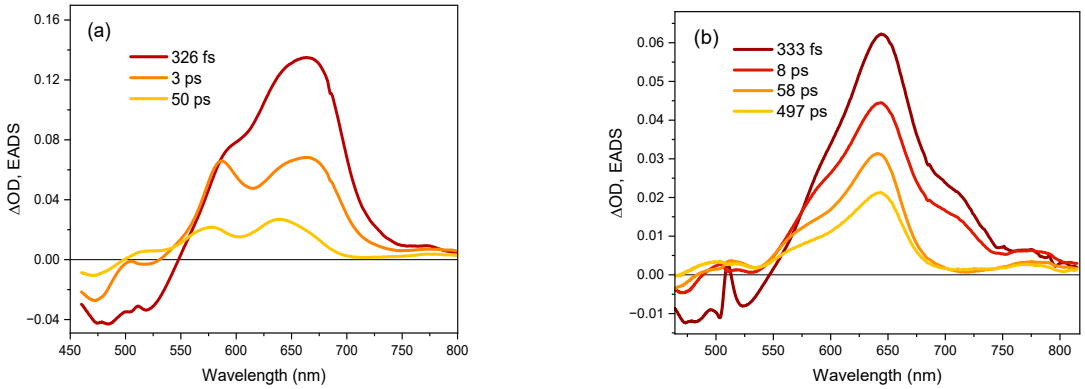


Figure S11. Evolution associated difference spectra (EADS) for **1** in (a) EtOH, and (b) THF.

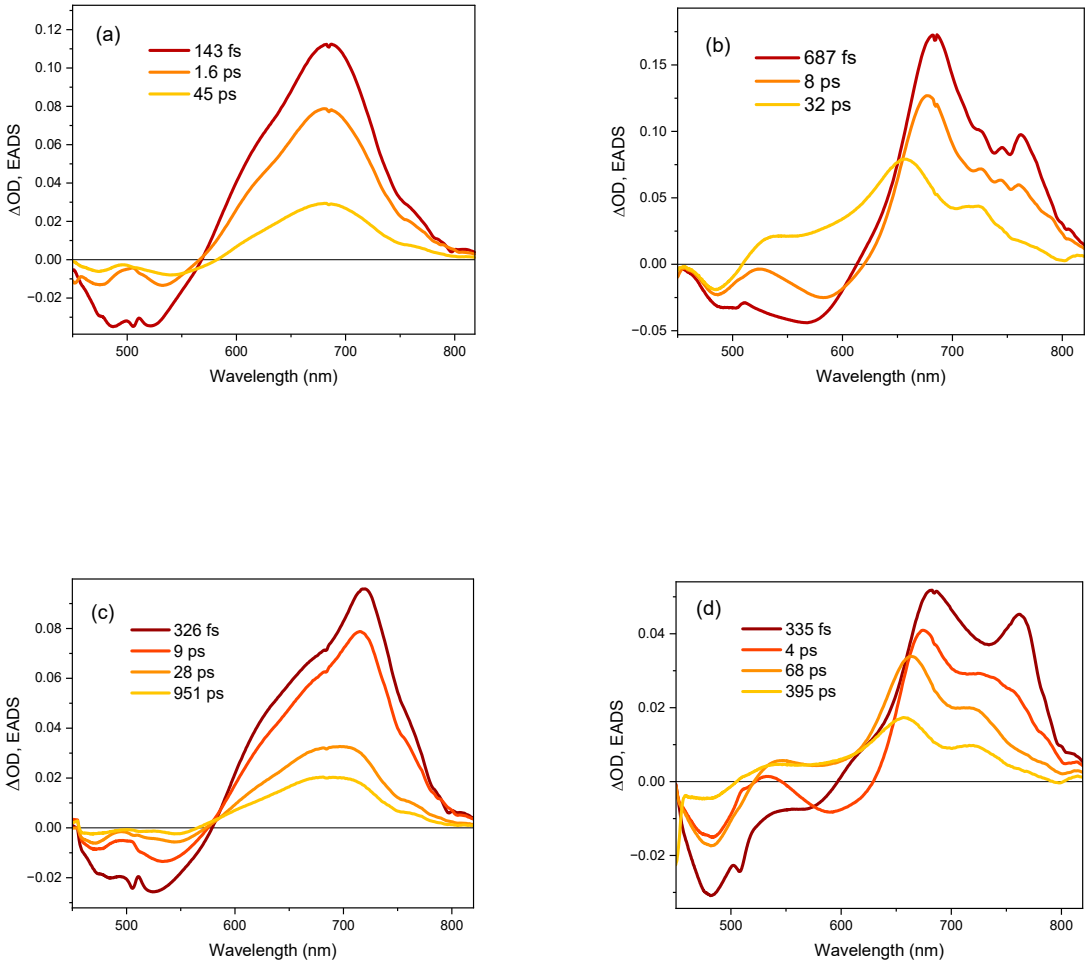


Figure S12. Evolution associated difference spectra (EADS) for (a) **2** and (b) **3** in EtOH, and (c) **2** and (d) **3** in THF. The EADS were obtained by global fit of the kinetic traces.

Optimised geometry of **1**

| | | | |
|---|---|---|---|
| C | 4.751199 | -2.09583 | 0.000053 |
| C | 5.34461 | -0.83173 | 0.00015 |
| C | 4.538583 | 0.296854 | 0.000108 |
| C | 3.134789 | 0.203431 | -2.6E-05 |
| C | 2.559134 | -1.07999 | -0.0001 |
| C | 3.357519 | -2.21572 | -5.7E-05 |
| H | 6.430495 | -0.75342 | 0.000249 |
| H | 5.006113 | 1.28225 | 0.000167 |
| H | 1.475632 | -1.17398 | -0.00015 |
| H | 2.896215 | -3.20534 | -0.00012 |
| O | 5.578522 | -3.17546 | 0.000128 |
| C | 2.355546 | 1.432394 | -0.00011 |
| H | 2.924286 | 2.365247 | -0.00021 |
| C | 1.013953 | 1.601813 | -0.00014 |
| C | 0.391996 | 2.954401 | -9.7E-05 |
| C | -1.11985 | 1.285991 | -7E-06 |
| N | 0.006878 | 0.632805 | -7.8E-05 |
| O | 0.880828 | 4.068096 | -0.00011 |
| N | -0.97283 | 2.667467 | 0.000002 |
| C | -2.00473 | 3.677276 | 0.000231 |
| H | -2.63271 | 3.602831 | 0.897991 |
| H | -1.49881 | 4.648336 | -0.00013 |
| H | -2.63341 | 3.602505 | -0.897 |
| C | -2.43912 | 0.672067 | 0.000024 |
| H | -3.2975 | 1.344298 | 0.000016 |
| C | -2.59352 | -0.66641 | -0.00011 |
| H | -1.69228 | -1.28166 | -0.0002 |
| C | -3.83684 | -1.39156 | -7.4E-05 |
| C | -4.06775 | -2.75432 | -0.00012 |
| H | -3.32168 | -3.54269 | -0.00027 |
| C | -5.99788 | -1.85232 | 0.000138 |
| H | -7.06933 | -1.68332 | 0.00025 |
| N | -5.40745 | -3.02882 | 0 |
| N | -5.10109 | -0.83301 | 0.000096 |
| H | -5.32383 | 0.149693 | 0.000185 |
| H | 5.057531 | -3.98299 | -0.0002 |

Optimised geometry of **2**

| | | | |
|---|---|---|---|
| C | -4.80213 | -2.33537 | -0.40841 |
| C | -3.40428 | -2.348 | -0.35547 |
| C | -2.69928 | -1.15733 | -0.24392 |
| C | -3.37476 | 0.074943 | -0.18248 |
| C | -4.7805 | 0.06063 | -0.23757 |
| C | -5.49366 | -1.12358 | -0.3491 |
| H | -2.86645 | -3.29708 | -0.40201 |
| H | -1.61246 | -1.16706 | -0.20256 |
| H | -5.3244 | 1.004872 | -0.19145 |
| H | -6.58152 | -1.1289 | -0.39133 |
| C | -2.69566 | 1.356444 | -0.06524 |
| H | -3.33578 | 2.241046 | -0.02653 |
| C | -1.37268 | 1.62746 | 0.004621 |
| C | -0.8593 | 3.020141 | 0.123854 |
| C | 0.776875 | 1.475679 | 0.075942 |
| O | -5.54063 | -3.47224 | -0.51746 |
| H | -4.9579 | -4.23576 | -0.54889 |
| C | 2.14314 | 0.965885 | 0.090126 |
| H | 2.942764 | 1.700507 | 0.173816 |
| C | 2.403331 | -0.34895 | 0.000668 |
| H | 1.544121 | -1.01796 | -0.08953 |
| C | 3.722641 | -0.98817 | 0.001666 |
| C | 4.929269 | -0.27472 | 0.100478 |
| C | 3.818622 | -2.38138 | -0.0911 |
| H | 4.920472 | 0.813343 | 0.188222 |
| C | 5.071558 | -2.98307 | -0.09234 |
| H | 2.912651 | -2.98475 | -0.1637 |
| C | 6.197846 | -2.16951 | 0.00375 |
| H | 5.177824 | -4.06443 | -0.16544 |
| O | -1.43522 | 4.089809 | 0.178245 |
| N | -0.29324 | 0.739984 | -0.01744 |
| N | 0.522685 | 2.837914 | 0.163652 |
| C | 1.47283 | 3.920491 | 0.277795 |
| H | 2.069039 | 3.829358 | 1.195073 |
| H | 2.140302 | 3.955288 | -0.59306 |
| H | 0.892849 | 4.848094 | 0.320056 |
| H | 7.198705 | -2.60516 | 0.005222 |
| N | 6.134853 | -0.83669 | 0.100981 |

Optimised geometry of **3**

| | | | |
|---|---|---|---|
| C | 5.304278 | -2.9984 | -6.9E-05 |
| C | 3.926791 | -2.75252 | -0.00026 |
| C | 3.450932 | -1.44879 | -0.00027 |
| C | 4.340581 | -0.35902 | -5.7E-05 |
| C | 5.720796 | -0.63295 | 0.000131 |
| C | 6.205991 | -1.93176 | 0.000124 |
| H | 3.224856 | -3.58876 | -0.00041 |
| H | 2.380262 | -1.25803 | -0.00037 |
| H | 6.427957 | 0.197348 | 0.000319 |
| H | 7.274829 | -2.13838 | 0.00028 |
| C | 3.908766 | 1.029402 | 0 |
| H | 4.701563 | 1.78135 | 0.000116 |
| C | 2.658561 | 1.546302 | 0.000004 |
| C | 2.413158 | 3.014231 | 0.000116 |
| C | 0.518526 | 1.800884 | -3.3E-05 |
| O | 5.822887 | -4.25458 | -7.2E-05 |
| H | 5.111356 | -4.90064 | -0.00015 |
| C | -0.91892 | 1.552106 | -6.7E-05 |
| H | -1.56875 | 2.426394 | -8E-06 |
| C | -1.41918 | 0.306059 | -2.7E-05 |
| H | -0.70178 | -0.51735 | -2E-06 |
| C | -2.83855 | -0.06759 | -5.9E-05 |
| C | -3.88013 | 0.876314 | -0.00051 |
| C | -3.17066 | -1.43108 | 0.000386 |
| C | -5.20737 | 0.474905 | -0.00047 |
| H | -3.65844 | 1.941854 | -0.00095 |
| C | -4.49537 | -1.85178 | 0.000423 |
| H | -2.37433 | -2.17493 | 0.000712 |
| C | -5.49553 | -0.88783 | 0.000012 |
| H | -6.02029 | 1.196421 | -0.0008 |
| H | -4.75923 | -2.90619 | 0.000763 |
| O | 3.177279 | 3.959892 | 0.000194 |
| N | 1.432841 | 0.874683 | -0.00012 |
| N | 1.020045 | 3.09484 | 0.000109 |
| C | 0.287308 | 4.340177 | 0.000171 |
| H | -0.33845 | 4.431969 | -0.89719 |
| H | -0.33857 | 4.43179 | 0.897466 |
| H | 1.029697 | 5.144801 | 0.000275 |
| N | -6.90258 | -1.31835 | 0.000062 |
| O | -7.12831 | -2.51643 | 0.000412 |
| O | -7.7597 | -0.45111 | -0.00026 |